Inelastic deuteron scattering from the high-spin isomer ^{178}Hf^{m2} (16^+)

S. Deylitz, B. D. Valnion, K. El Abiary, J. de Boer, A. Gollwitzer, R. Hertenberger, and G. Graw
Sektion Physik der Universität München, 85748 Garching, Germany

R. Kulessa
Institute of Physics, Jagellonian University, 30059 Cracow, Poland

Ch. Briançon, D. Le Du, and R. Meunier
Centre de Spectrométrie Nucléaire et de Spectrométrie de Masse-Orsay, 91405 Orsay, France

M. Hussonnois, O. Constantinescu, S. Fortier, J. B. Kim, L. H. Rosier, and G. Rotbard
Institut de Physique Nucléaire, F-91406 Orsay, France

Yu. Ts. Oganessian and S. A. Karamian
Joint Institute for Nuclear Research, Dubna, 101000 Moscow, Russia

H. J. Wollersheim, H. Folger, J. Gerl, and Th. Happ
GSI Darmstadt, D-64291 Darmstadt, Germany

C. Hategan
Institute of Atomic Physics, Bucharest, Romania
(Received 10 October 1995)

In inelastic scattering of 22 MeV deuterons from an isotope-separated target of ^{178}Hf containing about 2×10^{13} nuclei in the isomeric 16^+ state we observed rotational excitation to the 17^+ state at an excitation energy with respect to the isomeric state of 356.5 ± 0.4 keV and weak evidence for the 18^+ state at 737 ± 2 keV. We compared the differential cross sections with coupled-channel calculations and with scattering from ^{178}Hf (0^+) and ^{177}Hf ($7/2^-$).

PACS number(s): 25.45.De, 23.20.Lv, 24.10.Eq, 27.70.+q

I. INTRODUCTION

The high-spin isomer $I^\pi=16^+$ of ^{178}Hf at an excitation energy $E_x=2446$ keV with a half life time of $T_{1/2}=31$ yr [1–5] is unique with respect to stability of high angular momentum. The structure of this state is a pure, aligned four-quasiparticle configuration in a deformed potential ($\beta_2\approx0.25$), with two protons in the $\pi[404]7/2$ and the $\pi[514]9/2$ and two neutrons in the $\nu[514]7/2$ and the $\nu[624]9/2$ Nilsson orbitals. In this coupling scheme, the extremely low value of the excitation energy of a four-quasiparticle state and thus the stability of the 16^+ isomer results from a location of these Nilsson orbitals very close to the Fermi surface in ^{178}Hf and from the large and comparable values of their K quantum numbers. Due to the nature of aligned quasiparticle Nilsson orbitals with nearly identical quantum numbers one expects almost identical collective properties for the rotational band, built on the $K^\pi=16^+$ isomeric state and that on the $K^\pi=0^+$ ground state [6]. It is an experimental challenge to verify these predictions for this peculiar state. With this motivation the Hf isomer was produced in the ^{176}Yb(α,$2n$) reaction [7] with the high intensity ^{4}He beam (100 μA) at 36 MeV of the U 200 Cyclotron at Dubna. The ^{176}Yb target material was superenriched to 99.998% at the PARIS mass separator of CSNSM in Orsay. High purity chemistry methods were developed to recover the Hf isotopes from the target with an efficiency better than 90% [8,9]. The long lifetime of the isomer allows collection of material, preparation of targets, suitable for various experiments in different laboratories. Studies with collinear laser spectroscopy in Orsay by Boos *et al.* [10] yielded information on the rms radius, the magnetic moment and the spectroscopic quadrupole moment of the 16^+ isomeric state. The deduced magnetic moment $\mu_I=+8.16(4)\mu_N$ and intrinsic quadrupole moment $Q_0=7.2(1)$ b agree with theoretical expectation [6]. In a (p,t) reaction study by Rotbard *et al.* [11] the transition from the 16^+ four-quasiparticle state in ^{178}Hf to that one in ^{176}Hf has demonstrated significantly reduced cross section, in agreement with expected blocking due to the neutron-pair breaking.

To determine the moment of inertia of the rotational band, built on the $K^\pi=16^+$ isomeric state, inelastic proton and deutron scattering [9,12] at tandem energies and γ radiation following Coulomb excitation [13] was studied in Munich and at GSI, respectively. In these first experiments a target was prepared with only chemically separated Hf fraction, containing 2.1×10^{14} atoms of the isomer and also more than hundred times of other Hf isotopes, produced during the irradiation besides some other chemical impurities. In inelastic scattering of 22 MeV deuterons only a weak indication for the observation of a new excited state (tentatively assigned as 17^+) at an excitation energy near 353 keV above the

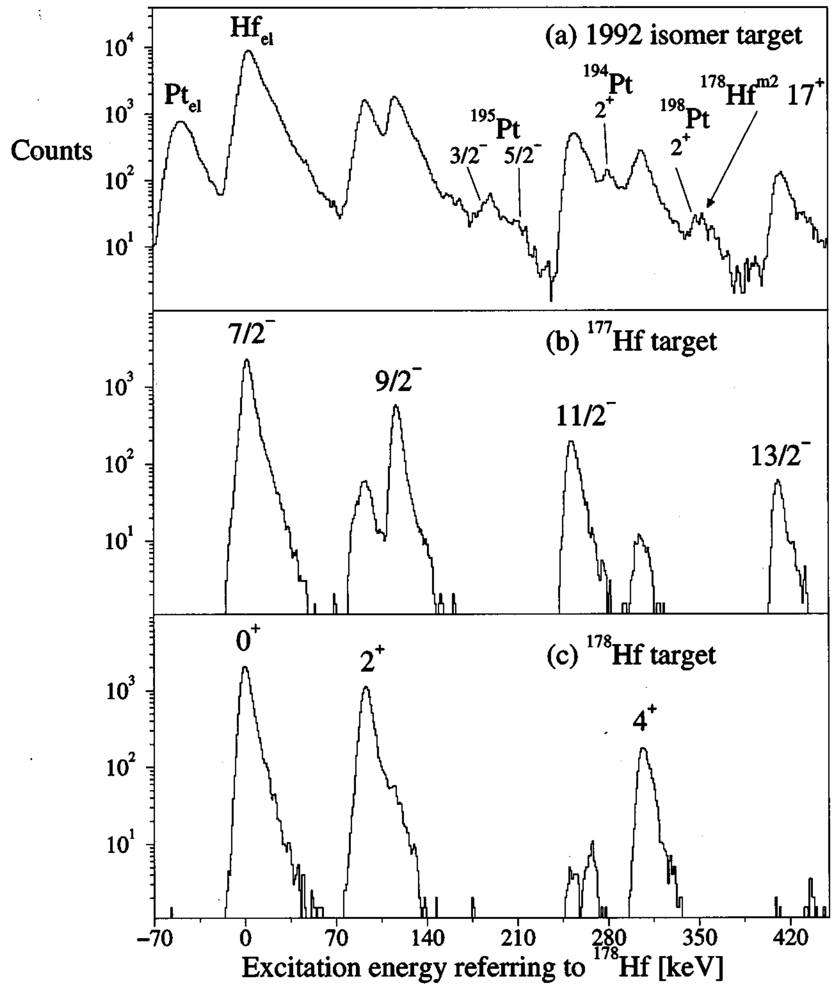

FIG. 1. Part of the spectra in 22 MeV deuteron scattering from different targets at $\theta_{lab}=100°$. The energy calibration is calculated from scattering on a mass 178 target. (a) was obtained using a target containing 2.1×10^{14} ^{178}Hf^{m2} (16^+) nuclei, (b) a 200 μg/cm^2 91.7% enriched ^{177}Hf, and (c) a 187 μg/cm^2 92.4% enriched ^{178}Hf target.

16^+ state was obtained from a spectrum at $\theta_{lab}=100°$ [9,12,15]. The result of Coulomb excitation, using a 4.77 MeV/u ^{208}Pb beam of the GSI Unilac, determining more precisely the excitation energy of this state as 357 keV, is presented in a paper parallel to this publication by Lubkiewicz *et al.* [13].

In this contribution, we report on a very recent experiment of inelastic deuteron scattering, using a mass-separated ^{178}Hf target, with an about 3% content of ^{178}Hf^{m2} (16^+). In spectra with about 6 keV full width at half maximum (FWHM) linewidth we observe the $16^+\rightarrow17^+$ transition at various scattering angles, determining the transition energy as $E_x=356.5\pm0.4$ keV and establish from the angular dependence the collective nature of this excitation.

II. EXPERIMENT

For inelastic scattering experiments at the Munich MP tandem accelerator we used the quadrupole–3 dipole (Q3D) high-resolution spectrograph with a detection solid-angle acceptance of 10.9 msr and a multilayer focal-plane detecting system [14], providing particle identification, focal-plane reconstruction [15], and background reduction due to particle selection. For 22 MeV deuterons, the detector accepts a range of excitation energy larger than 3 MeV with a linewidth of 6 keV FWHM or better, depending on target thickness, beam focusing, and long-term stability [16,19,20]. For the various Hf isotopes we did first experiments using proton, deuteron and α beams in the 100 to 500 nA range. Because of the unavoidable contamination of the isomeric ^{178}Hf target by heavy nuclei, we had to exploit the known kinematical energy shifts of the scattered particles at various scattering angles to obtain regions without lines from target contaminants in the relevant positions of excitation energy. It turned out that only for the scattering of deuterons near 22 MeV one can find ranges where background lines from target impurities are sufficiently low. In the following we discuss 22 MeV deuteron scattering only and we restrict the discussion to three experiments.

In the first we used as a target a non mass separated Hf fraction [called 1992 isomer target in Fig. 1(a)], containing 2.1×10^{14} ^{178}Hf^{m2} (16^+) nuclei electrosprayed on an area of about 5 mm diameter on a 30 μg/cm^2 carbon backing [see Fig. 1(a)]. The isomeric nuclei amount to about 3% of the

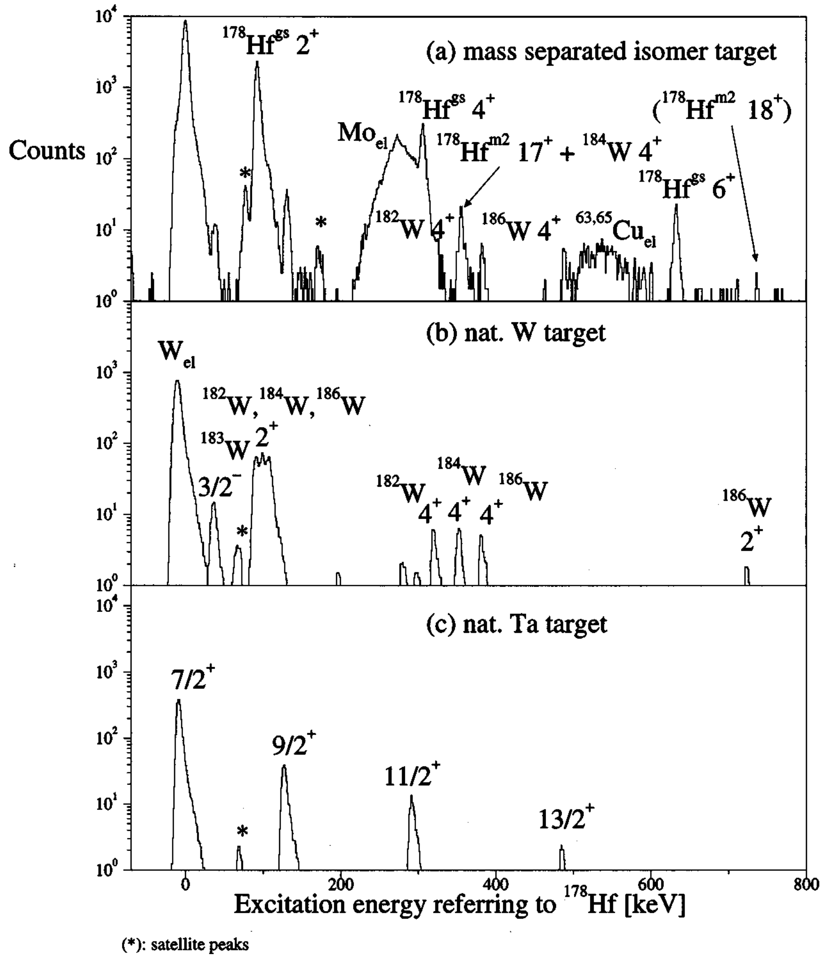

FIG. 2. Energy-calibrated spectra at $\theta_{lab}=68°$ for (a) the mass separated isomer target, (b) the natural W target, and (c) the natural Ta target (see Fig. 3 for details of the W and Ta contamination). Spurious satellite peaks indicated by an asterisk results from detector readout software [14,15].

^{178}Hf content in the target, the ^{177}Hf content of the target was even larger by a factor of a hundred compared to the isomer, and there were also some contributions from other Hf isotopes [11], all produced in the (α,xn) reactions on ^{176}Yb. The quantitative composition of the target has been determined using x-ray measurement [17]. In addition, we identified chemical impurities resulting from the chemical separation process, the heaviest ones being Pt, Zr, and Br (see below) [8,12].

In a second experiment [18–20] [see Figs. 1(b) and 1(c)] we studied the scattering from ^{177}Hf $(7/2^-)$ and from ^{178}Hf (0^+), using targets of evaporated Hf-oxide, 200 μg/cm^2 for ^{177}Hf, enriched to 91.7% and 187 μg/cm^2 for ^{178}Hf, enriched to 92.4%, on 20 μg/cm^2 carbon backings. Spectra were taken at laboratory angles between 15° and 100° in 2.5° steps (at full solid angle of the spectrograph). In these experiments the beam integration system and the detector efficiency allowed absolute cross section to be determined with 2% relative and 5% systematic accuracy.

In the third experiment [18–20] [see Fig. 2(a)], we used an isotopically separated target produced at the CSNSM PARIS separator [8] by direct implantation into a 40 μg/cm^2 carbon backing. Due to the production process, the target is free of other Hf isotopes and thin enough to yield spectra with high energy resolution. In the mass separation process at the focal plane, the beam spot of the ^{178}Hf$^+$ ions was sharply peaked horizontally and had a vertical extension of about 20 mm. A mask in front of the target limited the possible active area of the target to less than 2 mm by 4 mm. In the scattering experiment a horizontal deflection of the deuteron beam with a width of 1 mm showed that the width of the target-material distribution is possibly more narrow than the width of the beam. We thus had incomplete overlap of the beam with the target. From the fabrication process the ^{178}Hf^{m2} content is expected to be 3% of the ^{178}Hf (0^+) content of the target. In the experiment we observed an effective area density of 1.0 μg/cm^2 for ^{178}Hf (0^+) and thus 0.03 μg/cm^2 for ^{178}Hf^{m2}.

III. DATA EVALUATION

A. Excitation energies

Figures 1 and 2 show part of typical spectra for inelastic deuteron scattering, obtained in the respective experiments. They range from elastic scattering to an excitation energy up to 400 and 800 keV, including thus, e.g., the $13/2^-$ or the 6^+ state of the ground-state rotational band of ^{177}Hf and

^{178}Hf, respectively. Note the logarithmic scale and the absence of unphysical background. The scales in all these spectra are calibrated to refer to the positions of respective excitation energies relative to elastic scattering from ^{178}Hf. Note that the deuteron energies from elastic scattering from 0^+ state of ^{178}Hf and from elastic scattering from the isomeric 16^+ state coincide. For the positions of all the strong lines a polynomial fit of second degree [16,20] and kinematical calculations reproduce literature data within ± 0.5 keV. Compared to [9,12], the calibration of the spectrum in Fig. 1(a) includes the $13/2^-$ transition in ^{177}Hf, extracted from an improved focal-plane reconstruction-technique [15]. The spectra show the effects of target impurities. With the exception of the mass-separated isomer target there are reactions from the other Hf isotopes. Elastic scattering from these isotopes as well as from the isomeric state add up in the elastic Hf peak, causing for thicker target [Fig. 1(a)] some broadening and a shift due to the dominance of ^{177}Hf in this target. This target also shows elastic and inelastic scattering from Pt and contributions from lighter elements like Zr and Br, which do not show up in the energy range displayed in Fig. 1(a).

With the isotope-separated isomer target [Fig. 2(a)] we observe contributions from W, Ta, Mo, and Cu. They result from some sputtering and migration process of these unvoidable materials in the mass-separator facility [8]. The width of the lighter impurity lines in the (d,d') spectra result from kinematical broadening due to the $\pm 3°$ acceptance of the spectrograph. If the focal-plane reconstruction is arranged to reproduce elastic scattering of these very different masses of the target, then these broad lines sharpen up allowing a unique mass identification [20]. To correct for reactions from Ta and W we measured on targets of natural Ta and W at the same angles and in identical kinematic conditions [18,19]; Figs. 2(b) and 2(c) show the relevant spectra with the vertical scale adjusted to match the relevant W and Ta lines in Fig. 2(a).

In Figs. 1(a) and 2(a) all peaks are identified and understood with respect to their peak positions and strength by comparison with reference spectra. The spectrum in Fig. 2(a) shows an additional transition at $E_x = 356.5 \pm 0.4$ keV, which is assigned to rotational excitation of the 17^+ state from the 16^+ isomeric state. In this range of excitation energy there is some overlap with the transition to the $E_x = 364.0$ keV 4^+ state in ^{184}W, which has a comparable line strength as the $E_x = 396.8$ keV 4^+ transition in ^{186}W [see summed spectra at 61° and 68° in Fig. 3(a)]. Comparing the spectra of the mass-separated target [Fig. 3(a), top] and of the natural W target [Fig. 3(a), bottom] and their normalizations, using the well separated $3/2^-$ state of ^{183}W [Fig. 2(b)], we conclude that the ^{184}W (4^+) excitation represents $25 \pm 5\%$ of the peak assigned to ^{178}Hf^{m2} (17^+).

Taking into account the measurements at the three angles $\theta_{\rm lab} = 45°$, 61°, and 68° (where the kinematical behavior of contaminant lines provides reasonable conditions) we obtain for the 16^+ to 17^+ transition a weighted average of $E_x = 356.5 \pm 0.4$ keV for the excitation energy. The individual values agree within their uncertainties of ± 0.6 keV. The observation of the 17^+ state at $E_x = 356.5 \pm 0.4$ keV is in agreement with the observation of a peak near 353 keV from the first target, which results from a superposition of the 17^+ isomer state and the excitation of the 2_1^+ state in ^{198}Pt, which is expected somewhat below 353 keV in the scale of ^{178}Hf excitation. The determined excitation energy is very close to the 355.2 keV which results if a fit of all members of the rotational ground-state band according to the extended cranking model of Harris [21] is applied.

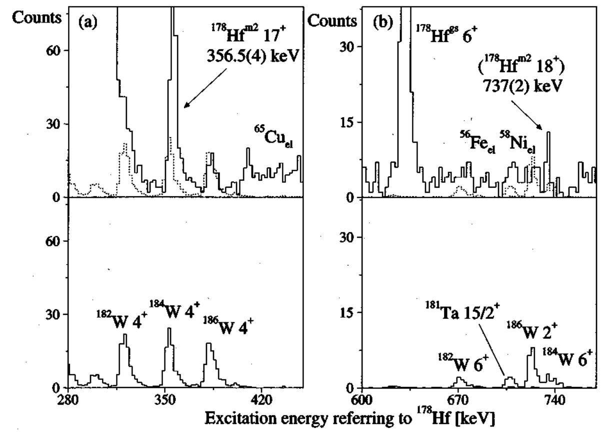

FIG. 3. Summed energy-calibrated spectra at 61° and 68° for the ^{178}Hf^{m2} (a) 17^+ and (b) tentatively assigned 18^+ state region (upper part) in comparison to contaminants (lower part).

Searching for the evidence of a 18^+ state, we observed a weak peak $E_x = 737 \pm 2$ keV. This observed excitation energy is not far away from $E_x = 734 \pm 1$ keV resulting for a 18^+ state if one assumes a constant moment of inertia in the isomeric band. The counting rate at the position $E_x = 737 \pm 2$ keV exceeds that one for the excitation of the $E_x = 748.3$ keV 6^+ state in ^{184}W [see Fig. 3(b)] and some continuous background caused by the lighter contaminants ^{56}Fe and ^{58}Ni.

B. Cross sections and coupled-channel calculations

In Fig. 4 we show the experimentally determined angular distributions of differential cross sections for scattering from ^{178}Hf, ^{177}Hf, and ^{178}Hf^{m2}. The data are compared with calculations for the rotational band members 0^+, 2^+, 4^+, 6^+, 8^+ in ^{178}Hf, $7/2^-$, $9/2^-$, $11/2^-$, $13/2^-$, and $17/2^-$ in ^{177}Hf, and 16^+, 17^+, 18^+ in ^{178}Hf^{m2}. Data of ^{177,178}Hf elastic scattering cross section are shown relative to the Rutherford cross section in order to display the reproduction of the absolute normalization. The data for the few lowest states of the ground-state rotational bands provide a clear pattern, allowing the verification of the optical potential and deformation parameters used in the calculations. The data points for the excitation of the 17^+ state in ^{178}Hf^{m2} are obtained, assuming a 3% content of metastable atoms in Hf and matching the intensity of the observed 2_1^+ state of ^{178}Hf with the predicted cross section of the coupled-channel calculations. In this way, we obtain an effective area content of 1 μg/cm^2 for ^{178}Hf (0^+) and 30 ng/cm^2 for ^{178}Hf^{m2} (16^+). The data point at $\theta_{\rm lab} = 100°$ results from the first measurement, using the isotopic composition given in Refs. [7] and [11], and subtracting some cross section for the 2^+ excitation, $E_x = 407.2$ keV, in ^{198}Pt, using the cross section ratio for 2^+ excitations of ^{194}Pt and ^{198}Pt from Ref. [22], the

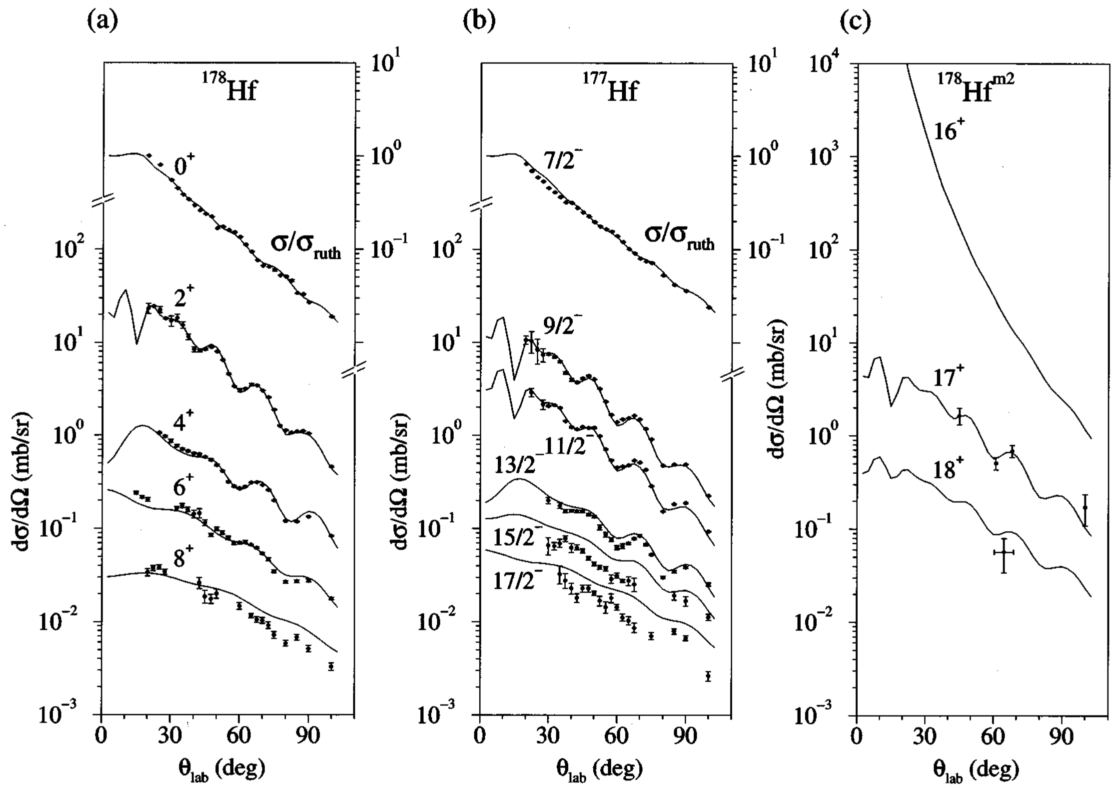

FIG. 4. Comparison of calculations in the coupled-channel approach with the experimental data: (a) optical parameters were extracted in a χ^2 fit to the ^{178}Hf (0^+) ground-state band data, (b) the calculations using these parameters are shown for the ^{177}Hf $(7/2^-)$ ground-state band, and (c) for the ^{178}Hf^{m2} (16^+) band. For the 18^+ state the tentatively assigned cross section of the summed spectra at 61° and 68° is also indicated.

isotopic abundance of natural Pt and the observed cross section for the 2^+ ^{194}Pt excitation in this spectrum.

The calculations of differential cross sections use the method of coupled channels realized in the code ECIS90 of Raynal [23] with the optical model of scattering from a static, axially symmetric deformed nucleus with an intrinsic orbital angular momentum projection K along the symmetry axis. Following the procedure for ^{154}Sm and ^{232}Th data of Refs. [24,25], we start out with a χ^2 fit of the ^{178}Hf ground-state band data using a global set of optical potential parameters for deuteron scattering from Daehnick and Childs [26] and collective deformation parameters β_2, β_4, and β_6 from Ogawa *et al.*, obtained from 65 MeV proton scattering [27]. We then allow small variations in the central potential (typically smaller than five percent), varying potential strength against potential geometry, and a 10% smaller value of the β_2 deformation, which is consistent with the larger radius of the deuteron potential compared to the proton potential. Taking into account the relation between isoscalar and electromagnetic deformation parameters β_2 and the demand for constant deformation length $\beta_2 r_c$ [28], our extracted values agree with the electromagnetic one of Ref. [29]. The final values of the parameters are given in Table I.

In the formalism of [30] the deformation of the radius in the Woods-Saxon potential parametrization causes higher-order transition terms, e.g., $\lambda = 4$ transitions from the β_2 deformation. The coupled-channel calculations include all transitions up to $\lambda = 6$ allowed by angular momentum coupling, including reorientation terms. Coulomb excitation is included using the prescription of the Coulomb corrections of the code. The typical Coulomb-nuclear interference minimum could not be resolved because of the target-backing contribution of ^{12}C and ^{16}O in the relevant range of small scattering angles. For ^{178}Hf we obtain a good reproduction

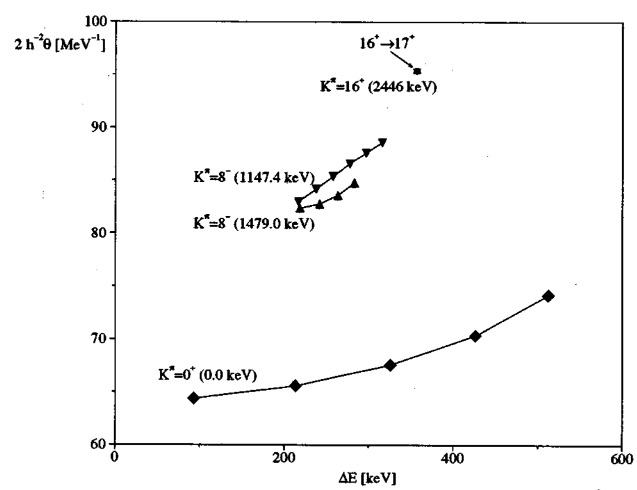

FIG. 5. Experimental values for the moments of inertia for the ground-state band, the two $K^\pi = 8^-$ bands, and the first transition in the $K^\pi = 16^+$ band of ^{178}Hf. The excitation energies of the band heads are given in parentheses.

TABLE I. Results of the χ^2 fit to the ^{178}Hf ground-state band data. Given in parentheses are the changes with respect to the parameter set of Refs. [26,27].

	Real pot.	Imaginary pot.	Spin-orbit pot.	Deformation
Depth	V_R=90.75 MeV (-3.5%)	W_S=0.603 MeV ($\pm$0%) W_D=12.87 MeV (+5.8%)	V_{LS}=6.69 MeV ($\pm$0%)	$\beta_2=+0.225$ (-8.9%) $\beta_4=-0.044$ ($\pm$0%)
Radius	r_0=1.22 fm (+4.3%) r_c=1.3 fm ($\pm$0%)	r_I=1.281 fm (-3.3%)	r_{LS}=1.07 fm	$\beta_6=+0.007$ (+16%)
Diffuseness	a_0=0.746 fm (+4.6%)	a_I=0.808 fm (-12.6%)	a_{LS}=0.808 fm ($\pm$0%)	

of the elastic scattering and of the 2^+ and 4^+ cross sections and a reasonable reproduction for the 6^+ and 8^+ states. This shows that a valid parametrization of the scattering potential and of quadrupole and hexadecapole transitions was obtained by only small variations of a well established set of parameters. With the parameters from ^{178}Hf, we calculate the $K^\pi=7/2^-$ rotational band in ^{177}Hf, changing the K value and the mass number only and obtain a perfect reproduction of the elastic scattering and of the excitation of the $9/2^-$ and $11/2^-$ states. The somewhat smaller experimental cross sections of the $13/2^-$, $15/2^-$, and $17/2^-$ might indicate a smaller β_4 deformation in ^{177}Hf due to the absence of one $7/2^-$ neutron. It should be noted that the elastic scattering cross sections differ significantly between ^{178}Hf and ^{177}Hf, especially due to the additional incoherent contributions from reorientation. The calculation for ^{177}Hf without any parameter adjustment serves a check for the K quantum number formalism to be treated correctly and that the quadrupole deformation is similar in these two nuclei.

Figure 4(c) shows the same type of calculation for the rotational-band members built on the $K^\pi=16^+$ isomeric state. Since the calculated [6] and observed [10] values of the intrinsic quadrupole moment Q_0 of the ground-state band and of the 16^+ state are almost identical, we used the value of β_2 from the ground-state band also for the isomeric band. For a better presentation of the experimental data, we show in Fig. 4(c) the elastic (16^+) and inelastic scattering cross sections in the same scale. For the states connected to the lowest state of the rotational band by angular momentum transfer $\lambda=2$ in a single step (the 2^+ for ^{178}Hf, the $9/2^-$ and $11/2^-$ for ^{177}Hf, the 17^+ and 18^+ for ^{178}Hf^{m2}) one observes a significant decrease of the excitation cross section with increasing initial angular momentum J. This is due to the different orientation of the intrinsic and the rotational angular momentum. The angular distribution of the 17^+ state has a pronounced oscillatory angular dependence reproduced by the experimental points. We take this agreement as evidence for $L=2$ transitions with a strength that matches a $K=16^+$ transition from $J^\pi=16^+$ to $J^\pi=17^+$ and a confirmation of the assumed β_2 deformation.

The predicted counting rate of the 18^+ state of 20 events agrees approximately with the observed 10 ± 4 events after subtracting the events of the ^{184}W (6^+) and the background from elastic scattering by ^{56}Fe and ^{58}Ni.

C. Moments of inertia

From the difference of excitation energies

$$\Delta E=\frac{\hbar^2}{2\theta}[J_f(J_f+1)-J_i(J_i+1)]$$

between the initial J_i and final state J_f moments of intertia are derived.

A comparison of the moments of inertia of the different K^π bands is shown in Fig. 5. The moment of inertia in the ground-state band is determined by superfluidity, increasing moments result from modifications of the pair-correlated properties with respect to the ground state [31]. This leads to the higher moments of the two two-quasiparticle $K^\pi=8^-$ bands and again the higher $(2/\hbar^2)\,\theta$ value of 95.4 ± 0.2 MeV^{-1} for the $16^+\rightarrow17^+$ transition (about a factor 1.5 with respect to the ground-state values in the low spin range) in the four-quasiparticle $K^\pi=16^+$ band. For the tentatively assigned $17^+\rightarrow18^+$ transition we obtain approximately the same value as for the $16^+\rightarrow17^+$ transition. The deduced moment of inertia of the $16^+\rightarrow17^+$ transition agrees within the errors with the one calculated according to Ref. [21].

IV. CONCLUSIONS

High-resolution particle spectroscopy in inelastic deuteron scattering established in ^{178}Hf^{m2} the 17^+ member of the rotational band at an excitation energy of $E_x=356.5\pm0.4$ keV above the 16^+ isomeric state and provides weak evidence for a possible candidate for the 18^+ state at $E_x=737\pm2$ keV. The observed cross sections are in agreement with calculations assuming the value for the isoscalar quadrupole transition matrix element the one derived for the ground-state band, in accordance with theoretical predictions and with the measured spectroscopic charge quadrupole moment of the 16^+ state. The moment of inertia deduced from the $16^+\rightarrow17^+$ transition is about 1.5 times larger than the moment of inertia of the ground-state band in the low-spin range.

ACKNOWLEDGMENTS

We thank Dr. H.J. Maier for the skillful preparation of targets and Dr. Th. Faestermann for his help in the operation of the Q3D magnetic spectrograph. This work was supported in part by the IN2P3-JINR collaboration agreement through the PICS 208, the DFG under II C4–Gr 894/2 and under Bo 1109/1 and by the Beschleunigerlaboratorium der Universität und der Technischen Universität München. One of us, C.H., appreciates support by the International Office in Karlsruhe.

[1] R.G. Helmer and C.W. Reich, Nucl. Phys. **A114**, 649 (1968).
[2] R.G. Helmer and C.W. Reich, Nucl. Phys. **A211**, 1 (1973).
[3] F.W.N. de Boer *et al.*, Nucl. Phys. **A263**, 397 (1976).
[4] T.L. Khoo *et al.*, Phys. Lett. **67B**, 271 (1977).
[5] J. van Klinken *et al.*, Nucl. Phys. **A339**, 189 (1980).
[6] P. Quentin *et al.*, in *Proceedings of the International Conference on Nuclear Shapes and Nuclear Structure at Low Excitation Energy,* Cargese, edited by M. Vergnes *et al.* (Plenum Press, New York, 1992).
[7] Yu. Ts. Oganessian *et al.*, J. Phys. G **18**, 393 (1992).
[8] M. Hussonnois *et al.*, CSNSM Scientific Report (1992 – 1994) p. 68; and (unpublished).
[9] Ch. Briançon *et al.*, in *Proceedings of the 8th International Symposium on Capture Gamma-Ray Spectroscopy and Related Topics*, Fribourg, edited by J. Kern (World Scientific, Singapore, 1994), p. 192.
[10] N. Boos *et al.*, Phys. Rev. Lett. **72**, 2689 (1994).
[11] G. Rotbard *et al.*, Phys. Rev. C **48**, R2148 (1993).
[12] Th. Happ *et al.*, Jahresbericht B.L. (1992), p. 65 and GSI Annual Report (1992), p. 91.
[13] E. Lubkiewicz *et al.*, GSI Scientific Report (1994), p. 36; and (unpublished).
[14] E. Müller-Zanotti, M. Bisenberger, R. Hertenberger, H. Kader, and G. Graw, Nucl. Instrum. Methods A **310**, 706 (1991).
[15] B.D. Valnion, Diploma thesis, Munich, 1992.
[16] R. Hertenberger, Ph.D. thesis, Munich, 1991.
[17] X-ray measurement by S. Zausser, Mainz (1992).
[18] S. Deylitz *et al.*, Bl Annual Report, Munich (1994).
[19] S. Deylitz, Diploma thesis, Munich, 1995.
[20] B.D. Valnion, Ph.D. thesis, Munich, 1996.
[21] S.M. Harris, Phys. Rev. B **138**, 509 (1965).
[22] P. Mukherjee *et al.*, Nucl. Phys. **64**, 65 (1965).
[23] Extended version of code ECIS90 by J. Raynal, C.E.N. Saclay (1990).
[24] H. Clement, R. Frick, G. Graw, F. Merz, P. Schiemenz, and N. Seichert, Phys. Lett. **116B**, 109 (1982).
[25] H. Clement, R. Frick, G. Graw, F. Merz, H.J. Scheerer, P. Schiemenz, N. Seichert, and Sun Tsu Hsun, Phys. Rev. Lett. **48**, 1082 (1982).
[26] W.W. Daehnick, J.D. Childs, and Z. Vrcelj, Phys. Rev. C **21**, 2253 (1980).
[27] H. Ogawa *et al.*, Phys. Rev. C **33**, 834 (1986).
[28] V.A. Madsen *et al.*, Phys. Rev. C **12**, 1205 (1975).
[29] S. Raman *et al.*, At. Data Nucl. Data Tables **36**, 1 (1987).
[30] T. Tamura, Rev. Mod. Phys. **37**, 679 (1965).
[31] A. Bohr and B.R. Mottelson, *Nuclear Structure* (Benjamin, New York, 1975), Vol. 2, p. 37.